OBSERVATIONS OF SEVERE CONVECTION AND ENVIRONMENTAL CONDITIONS 15 MAY 1986

John E. Wright

National Weather Service Office
Purdue University
West Lafayette, Indiana

Abstract

A case study was done for the 15 May 1986 severe thunderstorm and tornado mini-outbreak over southwest Indiana. Storm types and environmental conditions were analyzed to check for predictability with current severe storm knowledge and conceptual ideas. Environmental conditions preceding and during the severe weather outbreak were investigated with soundings and hodographs. A radar analysis exposed reflectivity notches, hooks and bows associated with some of the storms.

Environmental conditions were found to destabilize as afternoon Convective Available Potential Energy (CAPE), B+, increased significantly. This helped to offset decreases in storm relative helicity which occurred during the afternoon. An old thunderstorm outflow boundary from a mesoscale convective system (MCS) provided a source of baroclinically generated horizontal vorticity as thunderstorm inflow was tilted upward by the updrafts producing mesocirculations. Both classic and high precipitation (HP) supercell storm types produced the severe weather over southwest Indiana. Rear inflow notches (RINs), weak echo notches (WINs) and hooks were common storm features observed.

1. Introduction

Severe convection produced tornadoes and damaging winds during the afternoon and evening hours of 15 May 1986 over southwest Indiana. Tornadic thunderstorms also occurred over parts of central Indiana and southwest Missouri (Storm Data 1986). Severe flash flooding occurred over southeast Missouri and extreme southern Illinois. This study presents the environmental conditions and selected radar observations of the storms in southwest Indiana.

The severe weather occurred during a six hour period in southwest Indiana. Tornado watches were issued for the area by the National Weather Service (NWS), National Severe Storms Forecast Center (NSSFC). Two F0-scale tornadoes, two F2-scale tornadoes and one F1-scale tornado were confirmed. Corresponding wind speeds are 40-72 mph (F0), 73-112 mph (F1), and 113-157 mph (F2) (Fujita 1971). Path lengths of the tornadoes in southwest Indiana were short and narrow. Additionally, four damaging wind reports were received. Six injuries and at least 66,000 dollars worth of damage occurred in southwest Indiana. Tornado and wind damage reports are shown in Fig. 1.

2. Data

Rawinsonde data for Salem, Illinois (SLO) at both 1200 UTC 15 May 1986 and 0000 UTC 16 May 1986 were obtained from the National Climatic Data Center. Salem is located 81 nautical miles (n mi) northwest of Evansville. The data were input into the Skew-T/Hodograph Analysis and Research Program (SHARP) developed by Hart and Korotky (1991). Sounding plots, hodographs, convective indices and storm environment were the output from SHARP used in this case study. A modified 1200 UTC 15 May hodograph was produced by substituting radar observed storm motion of 239° at 40 knots (kts) for the predicted storm motion. The 0000 UTC 16 May hodograph was modified by substituting the radar observed storm motion of 240° at 40 kts for the predicted storm motion. Additionally, a run of data through SHARP was made to check the environmental stability of the atmosphere in northwest Kentucky where

Fig. 1. Map of storm damage reports for 15 May 1986 severe weather outbreak.

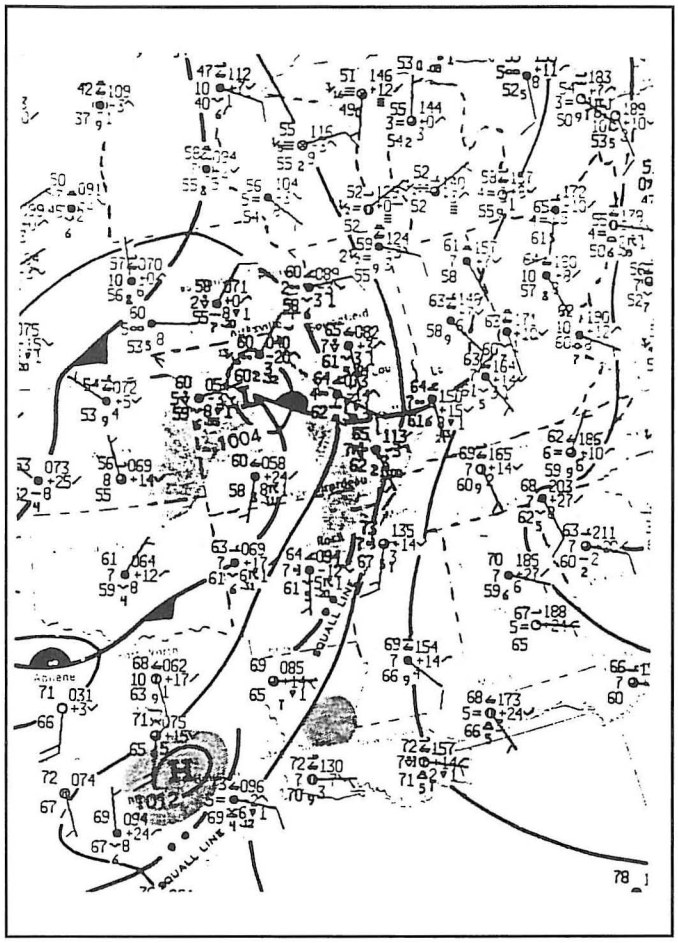

Fig. 2. Surface analysis for 1200 UTC 15 May 1986.

the storms initiated. The input data were modified with a surface temperature of 80° F, a surface dewpoint of 66° F and radar observed storm motion of 230° at 40 kts. Operational use of hourly NWS, AFOS Data Analysis Programs (ADAP) have been shown by Bothwell (1989) to be effective in predicting convection. Hourly surface data were used as input into ADAP to derive a mesoanalysis. Archived low-level reflectivity data were also obtained on 16mm photographic film for the network radar site at Evansville, Indiana. Elevation angle was set at 0.5°. The radar is a 10 cm wavelength Weather Surveillance Radar (WSR-57) with a two degree half-power beamwidth.

3. Environmental Conditions

At 1200 UTC 15 May 1986, the NWS, National Meteorological Center (NMC) surface analysis (Fig. 2) indicated a 1004 mb low pressure system centered over central Missouri. A warm front extended east southeast from the low pressure center to near Evansville and Louisville. A cold front extended south, southwest from the low to near Fort Smith, in west central Arkansas. High temperatures in the warm sector reached the upper 70's and lower 80's with dewpoints in the mid and upper 60's. Additionally, a mesoscale convective system (MCS) produced a quasi-stationary outflow boundary oriented from southwest to northeast across the Evansville area of southwest Indiana. A roll cloud resulting from the outflow boundary was visible from Evansville's Dress Regional Airport (Fig. 3). The MCS had accelerated from southern Illinois into southwest Indiana as a bow echo before stalling over the Evansville area.

The 1200 UTC sounding for Salem, Illinois (SLO) is shown in Fig. 4a. The sounding indicated deep layers of moist air from the surface up to near 500 mb. Deeper layers of moist air have been found in proximity to severe weather episodes over the Ohio Valley (Schaefer and Livingston 1990). The deep layers of moist air indicated by the 1200 UTC sounding differs from the mid-level dryness of "loaded gun" soundings found

Table 1. Convective indices and storm environment. Indices and environmental data based on Salem (SLO), Illinois sounding for both 1200 UTC 15 May and 0000 UTC 16 May 1986. Abreviations include surface (sfc), temperature (T), and dewpoint (TD).

	1200 UTC	MODIFIED (storm motion) 1200 UTC	0000 UTC	MODIFIED (sfc T, TD, storm motion) 0000 UTC	MODIFIED (storm motion) 0000 UTC
CAPE, B+ (j kg^{-1})	52	52	1,188	2,015	1,188
LI	+1	+1	−3	−5	−3
CAP STRENGTH (°C)	1.3	1.3	0.0	0.0	0.0
MAX UVV (m s^{-1})	10	10	49	63	49
EL (ft)	15,300	15,300	36,200	36,200	36,200
STORM MOTION (°/kts)	237/30 (predicted)	239/40 (observed)	282/27 (predicted)	230/40 (observed)	230/40 (observed)
BRN	0	0	12	26	12
SR HELICITY (0–3km) (m^2 s^{-2})	397	427	189	−61	−60
POS. SHEAR (0–2km) (10^{-3} s^{-1})	11.0	11.0	6.7	6.8	6.7

in Miller's (1972) mean tornado sounding common to the Great Plains. Strong veering of winds below 800 mb indicated low-level warm air advection, which is favorable for destabilizing the air mass. The 0000 UTC 16 May sounding for Salem is shown in Fig. 4b. A drier intrusion of air from 700 mb to 550 mb is apparent, which increased the potential for severe convection. However, significant moisture remained below 700 mb. Additionally, backing winds with height above 500 mb on the 0000 UTC sounding indicated cold air advection. Ambient temperatures above 500 mb had decreased about 2° F by evening. Sounding data were analyzed with SHARP. Output of the convective indices and storm environment are shown in Table 1. Computation of convective indices indicated a destabilization of the air mass, with a LI of 1 at 1200 UTC decreasing to −3 by 0000 UTC 16 May. A modified 0000 UTC sounding more representative of northwest Kentucky, where the severe convection initiated, was produced using a surface temperature of 80° F and a dewpoint of 65° F. The modified sounding yielded a LI value of −5 over northwest Kentucky. Diurnal (surface) temperature fluctuations, warm air advection below 800 mb, and cold air advection above 500 mb contributed to the increased instability. The Convective Available Potential Energy (CAPE), B+, significantly increased from a morning value of 52 j kg^{-1} to an evening value of 1,188 j kg^{-1}, further indicating the degree of increased instability. Again, looking at Table 1 the modified evening sounding data indicated even greater instability of the air mass over Kentucky with a B+ value of 2,015 j kg^{-1}. Cap strength at 1200 UTC was 1.3° C decreasing to 0° C by 0000 UTC. Estimated potential maximum updraft (MAX UVV) strength increased from 10 m s^{-1} at 1200 UTC to 49 m s^{-1} by 0000 UTC 16 May 1986. Modified 0000 UTC output indicated potential MAX UVV strength of 63 m s^{-1} over northwest Kentucky. Equilibrium level (EL) increased from 15,300 ft above ground level (AGL) at 1200 UTC to 36,200 ft (AGL) at 0000 UTC 16 May.

Numerical simulations have shown that vertical shear of the environmental wind is an important factor in determining observed and modeled storm structure (Weisman and Klemp 1982). Strong winds of 40 to 60 kts at and above 900 mb on the 1200 UTC sounding indicated potential for damaging winds in thunderstorms. An overall decrease in wind speeds below 500 mb was noted by 0000 UTC 16 May. Weisman and Klemp (1982, 1984) have shown that much of the relationship between storm type, wind shear, and buoyancy can be represented in the form of a Bulk Richardson Number (BRN). Computation of the BRN, which takes buoyancy and shear into account, indicated an increase in values from 0 in the morning to 12 by 0000 UTC. Weisman and Klemp (1984) found that supercells formed when the BRN was low. The 0000 UTC 16 May BRN value of 12 fell within the range of 10 to 40 found by Weisman and Klemp to most likely favor supercell type storms.

The hodograph for 1200 UTC 15 May 1986 is shown in Fig. 5a and 0000 UTC 16 May is shown in Fig. 5b. A modified hodograph for 0000 UTC is shown in Fig. 5c. The storm motion in the modified 0000 UTC hodograph was changed from the predicted storm motion of 282° at 27 kts to the radar observed storm motion of 230° at 40 kts. Storm relative (sr) helicity (Lilly 1986; Davies-Jones et al. 1990) is a parameter for measuring rotational potential in the low-level windfield. The SHARP program estimates of sr helicity (0–3 km, AGL) ranged from 397 $m^2 s^{-2}$ at 1200 UTC to 189 $m^2 s^{-2}$ at 0000 UTC 16 May. Substitution of the radar observed storm motion, 239° at 40 kts, for the predicted storm motion, 237° at 30 kts, increased the sr helicity to 427 $m^2 s^{-2}$ at 1200 UTC. A preliminary study (Davies-Jones et al. 1990) revealed the rough ranges of helicity

Fig. 3. Photo looking west from Evansville area at a roll cloud associated with an outflow boundary generated by an MCS during the early afternoon of 15 May 1986.

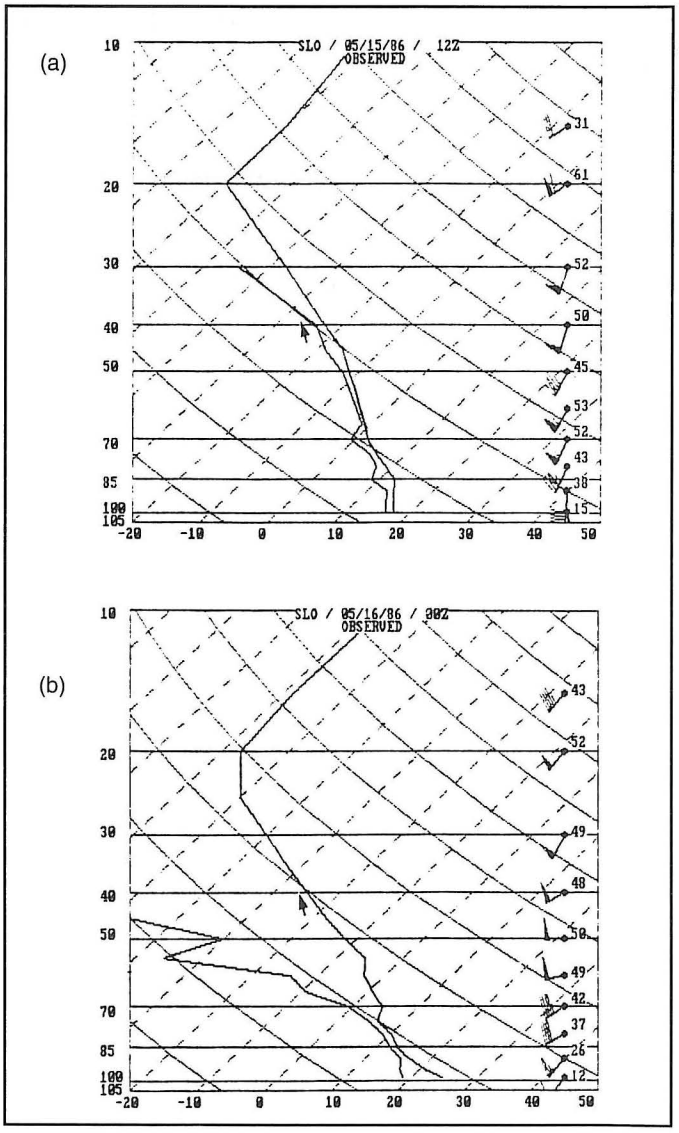

Fig. 4. Salem (SLO), Illinois sounding: (a) observed 1200 UTC 15 May 1986 and (b) observed 0000 16 May 1986. Left column of sounding shows pressure levels of wind plots in tens of mb. Units of wind barbs are in kts.

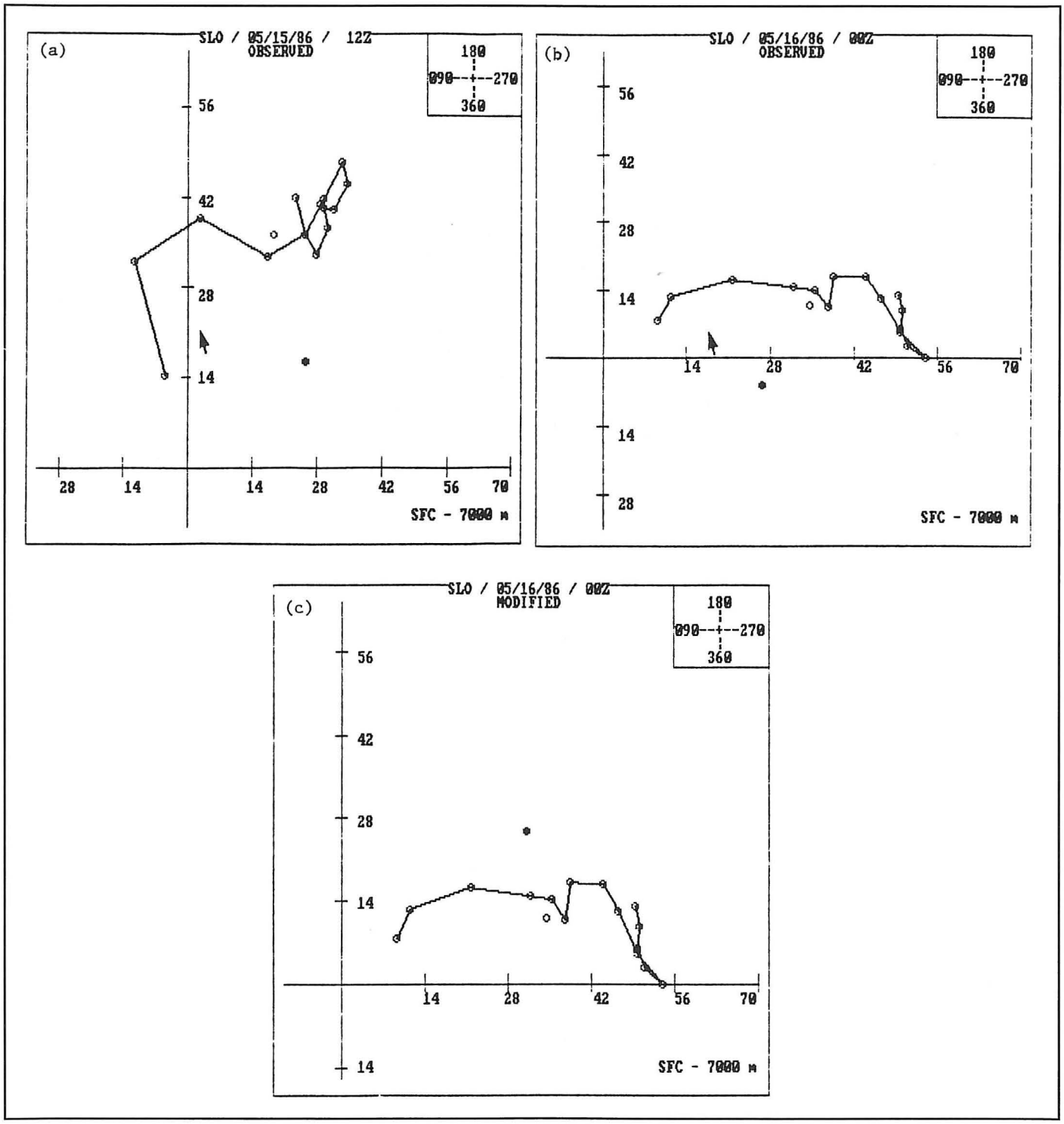

Fig. 5. Salem (SLO), Illinois hodograph: (a) observed 1200 UTC 15 May 1986, (b) observed 0000 UTC 16 May 1986 and (c) modified 0000 UTC 16 May 1986. Hodograph levels correspond to RAOB vertical wind levels (direction/kts, MSL), surface to 7,000 meters in 500 meter increments. The closed circle is the head of the storm motion vector and the open circle is the head of the 0–6 km (AGL) mean wind vector.

for weak, strong and violent tornadoes are 150–299, 300–449, and 450 or greater, respectively. Applying these ranges to the Salem, Illinois sr helicity estimates, the potential for weak to strong tornadoes was indicated. However, computed sr helicity values were less favorable by 0000 UTC. In fact, the modified hodograph produced a -60 m^2 s^{-2} when the radar observed storm motion, 230° at 40 kts, was substituted for the predicted motion, 282° at 27 kts. Still, two strong (F2) tornadoes were confirmed in southwest Indiana and another two in southeast Missouri. Examination of the 1200 UTC hodograph for Salem revealed clockwise turning through 6,000 ft (AGL) which favors supercell type storms with cyclonically rotating meso-

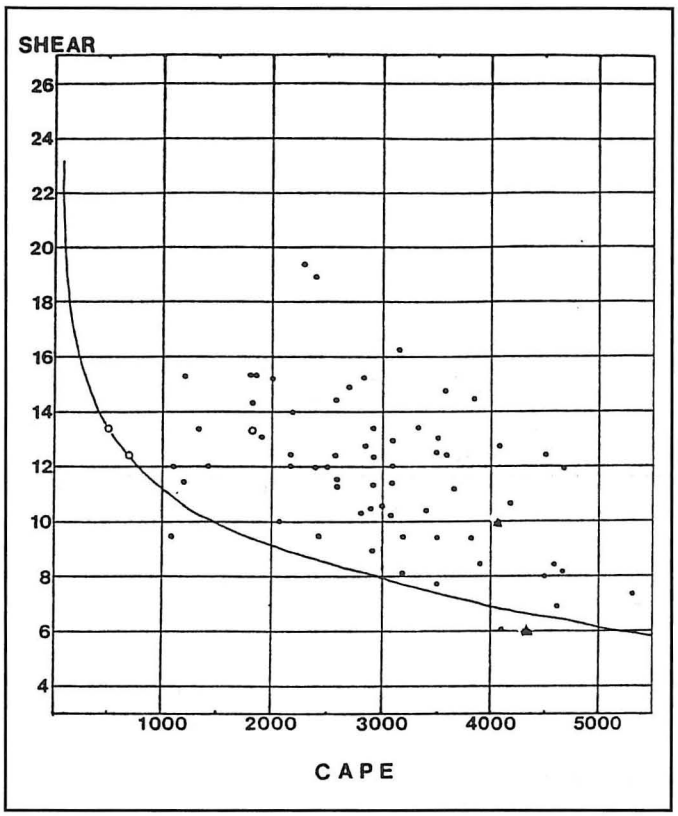

Fig. 6. Scatter diagram showing the relationship between Convective Available Potential Energy (CAPE) and 0–2 km (AGL) positive wind shear for the 69 warm season (May 15 to Aug. 31) tornado cases. Solid curved line is a suggested lower limit of combined CAPE/low-level shear value that would support the development of strong or violent mesocyclone-induced tornadoes. The non-shaded circles represent tornado cases associated with tropical cyclones. The non-shaded triangles represent tornado cases associated with derechos.

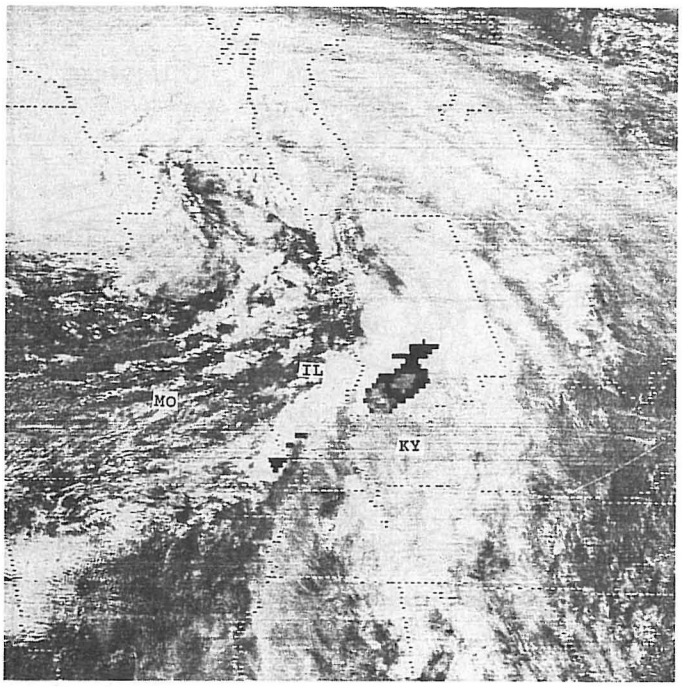

Fig. 7. Infrared satellite image for 2201 UTC 15 May 1986, using C3 curve enhancement.

cyclones. Clockwise turning of the hodographs is less impressive on both the observed and modified hodographs for 0000 UTC 16 May.

Davies (1989) suggested that the positive shear calculation is an effective way of quantitizing rotational potential from hodographs. The case studies in Davies (1989) paper suggested that a sounding derived analysis of the 0–2 km positive shear field could have valuable diagnostic potential for the severe weather forecaster operationally. Meteorologists must consider both the atmospheric stability and low-level wind shear when assessing the potential for severe convection, especially tornadogenesis. Variations in the combinations of wind and instability parameters associated with strong to violent tornadoes were studied by Johns et al. (1990). They found that during severe weather episodes limited instability can be compensated for by strong shear, a common scenario during the winter and spring months (cool season). In contrast, weaker wind shears can be compensated for by greater instability, a situation common during the months of summer (warm season). Numerical models suggest that wind shear and buoyant energy compensate for each other to some degree in the development of mesocyclone-induced tornadoes (Weisman and Klemp 1986). Using a CAPE, B+, value of 1,188 j kg^{-1} from the 16 May 0000 UTC sounding and a positive shear of 6.7 $\times$ 10^{-3} s^{-1} with the warm season scatter diagram (Fig. 6) developed by Johns et al. (1990), conditions would be considered marginal for strong tornadoes. Positive shear had diminished from the 11 $\times$ 10^{-3} s^{-1} computed for 1200 UTC 15 May.

Infrared satellite imagery for 2201 UTC 15 May is shown in Fig. 7. Convective cloud top temperatures were coldest, -55 to $-66°$ C, near Evansville in southwest Indiana. A decrease in cloud top temperatures had occurred since 2031 UTC on the tail portion of a developing comma cloud. By this time the thunderstorms had already spawned tornadoes in southwest Indiana. Studies by Xiang and Beckman (1986) showed that surface moisture convergence is maximized at the tail portion of vorticity comma clouds, where severe weather is most likely to develop. Mesoanalysis from 2200 to 2300 UTC (Fig. 8a-b) indicated surface moisture convergence maximums of 20 to 30 g kg^{-1} hr^{-1} $\times$ 10 over the southwest corner of Indiana and south central Missouri. This region of surface moisture convergence is linked to the warm frontal boundary and comma tail cloud. Both the warm front and MCS outflow boundaries served as sources of baroclinically generated horizontal vorticity as storm inflow was tilted into the vertical by the storms updraft. Maddox et al. (1980) developed a physical model of subcloud wind profiles near thermal boundaries to explain intensification of storms interacting with warm fronts or old thunderstorm outflow boundaries. This study by Maddox et al. attributed intensification of the storms to greater wind shear and convergence along the pre-existing boundaries. Klemp (1987) found by modeling that outflow boundaries also serve as sources of baroclinically generated horizontal vorticity, which can be tilted into the vertical by a storm's updraft. In this case study, the interaction of the storms with the boundaries favored tornado production over southwest parts of Indiana. By 0000 UTC 16 May, the surface moisture convergence had weakened in southwest Indiana, and increased in south central Missouri. This increase in Missouri preceded and coincided with the tornado outbreak in southeast parts of that state.

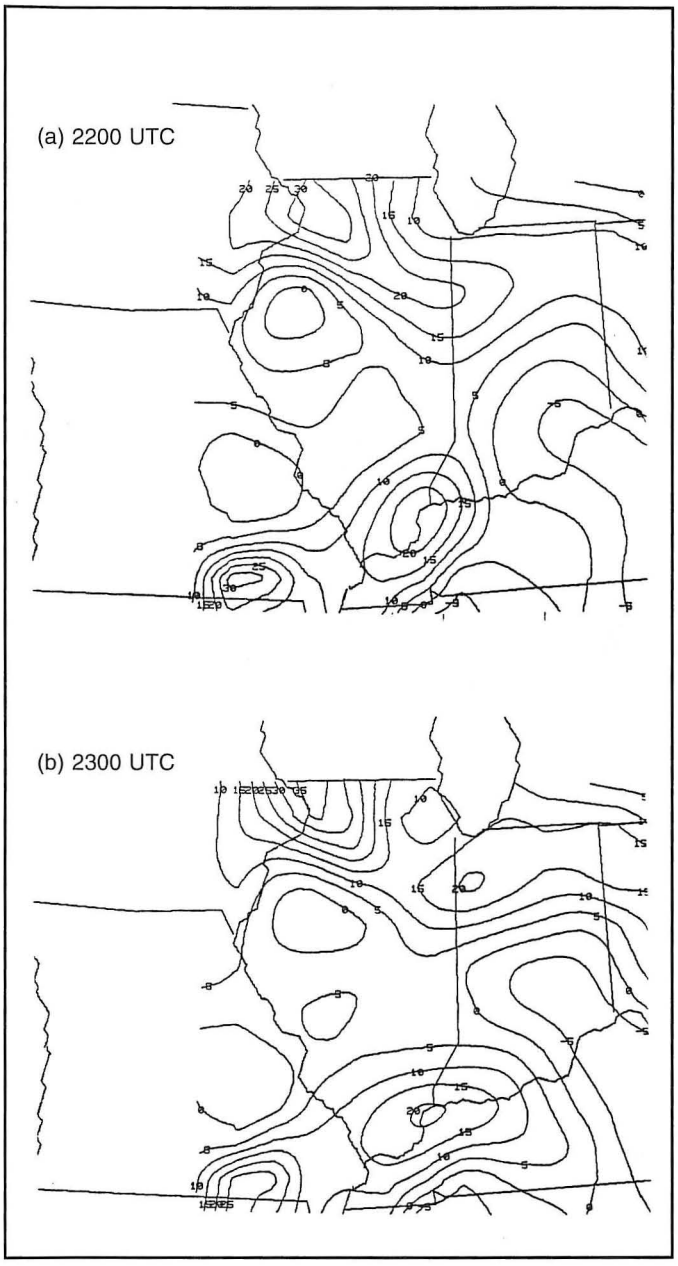

Fig. 8. Surface moisture flux convergence at (a) 2200 and (b) 2300 UTC 15 May 1986. Values shown are in tens of g kg^{-1} hr^{-1}.

4. Low-Level Reflectivity

Two sequences of radar tracings were made from 16mm radar film. The sequences were made for the time frames 2118 to 2128 UTC (Fig. 9a-d) and 2134 to 2151 UTC (Fig. 10a-e). These times were selected for greater film resolution when the range was 50 n mi. Video Integrator Processor (VIP) levels 1, 2, 3, 4, and 5 are contoured, and VIP 4 levels are shaded in black. The elevation angle was set at 0.5° for all tracings. The most impressive storms are labeled, A–F and possible mesocirculations labeled, M1–M9.

Prior to 2118 UTC, an MCS moved into southwest Indiana. The MCS produced wind damage at Blairsville, Indiana about 1855 UTC and later at 1915 UTC one n mi northeast of Stacer, Indiana. The MCS continued to travel east, southeast along the warm frontal boundary. Eastward movement of the MCS appeared to stall on the west and north sides of Evansville. The MCS outflow boundary appeared to provide a source of increased mesoscale moisture content and convergence. This outflow boundary also served as a source of baroclinically generated horizontal vorticity, which was tilted into the vertical by the storm updrafts to produce tornadic thunderstorms. Unfortunately, mid- and upper level cloudiness on the infrared satellite imagery concealed the probable boundary. A roll cloud or gust front cloud was observed from the Evansville airport looking northwest (Fig. 3).

By 2118 UTC (Fig. 9a), intense convective storms, A, B, and C, were moving northeast into the southwest corner of Indiana. Storm movement was from 230° at 40 kts. Low-level reflectivity patterns, time continuity and damage provided evidence of twin classic supercells, B and C. Both storms had sharp reflectivity gradients on the south and west flanks. Also, both storms had well defined hook echoes on the southwest flanks at times during the radar sequences. Storm B had at least a VIP 4 core reflectivity, while storm C had a VIP 5 core. The low-level reflectivity characteristics exhibiting a pendant or possible hook on the southwest flank of storm B suggested a probable mesocirculation, M1. A few minutes before this sequence storm C had indications of a hook echo on the southwest flank, indicating a probable second mesocirculation, M2. Also, it is evident that weak echo notches (WENs) developed on the southern flanks of each storm, B and C, from 2118 to 2128 UTC (Fig. 9a-d). Types of classic supercells may have more than one WEN or updraft as indicated in the low-level reflectivity pattern of storm C (Moller et al. 1990; Nelson 1987; Przybylinski et al. 1993). In fact, as the notches intruded into the higher VIP levels of storm C (2121 to 2123 UTC) two mesocirculations, M2 and M3, appeared to be highlighted. The larger size of storm C and it's inflow notches may have indicated greater potential for severe weather, but storm B produced wind damage first at 2125 UTC in the far southwest corner of Indiana. Storm C apparently had an unobstructed source of moist, unstable air from the south, southeast, while storm B competed for inflow with storm C and other convection to the southeast. The reflectivity pattern of storm B also suggested possible multiple updrafts, or inflow notches on the east and southeast flanks from 2118 to 2128 UTC. High-reflectivity cores (40 dBz and greater) in storms block the ambient flow through the core, but accelerate the flow on either side of the core (Brown and Crawford 1972). This produces a radial velocity pattern with centers of high velocity areas within the storm adjacent to the blocking core. Downwind notches on the northeast flanks of storms B and C at 2118 UTC and other times could have resulted from precipitation being carried downwind on either side of the high-reflectivity cores. Estimated ambient flow in the air at 20,000 ft (AGL) was from about 245° at 48 kts.

Two other storms, A and D, are also worth noting. No damage was confirmed from storm A, however, nearly classic supercell characteristics were observed in the low-level reflectivity pattern. An impressive reflectivity gradient can be seen on the south and east flanks at 2118 UTC. A VIP 5 core was present at 2118 UTC, which later weakened to a VIP 4 as splitting appeared to begin. Storm A had the maximum observed echo top, 40,000 ft (AGL), for the 2128 UTC network radar observation. The echo pattern of storm A at 2118 UTC suggests a possible pendant and mesocirculation, M4, on the southwest flank. Storm A appeared to evolve from classic to high-precipitation (HP) supercell characteristics between 2123 and 2134 UTC (Figs. 9c-d and 10a). Moller et al. (1990) found similar evolution of classic supercells to HP supercells in a study of

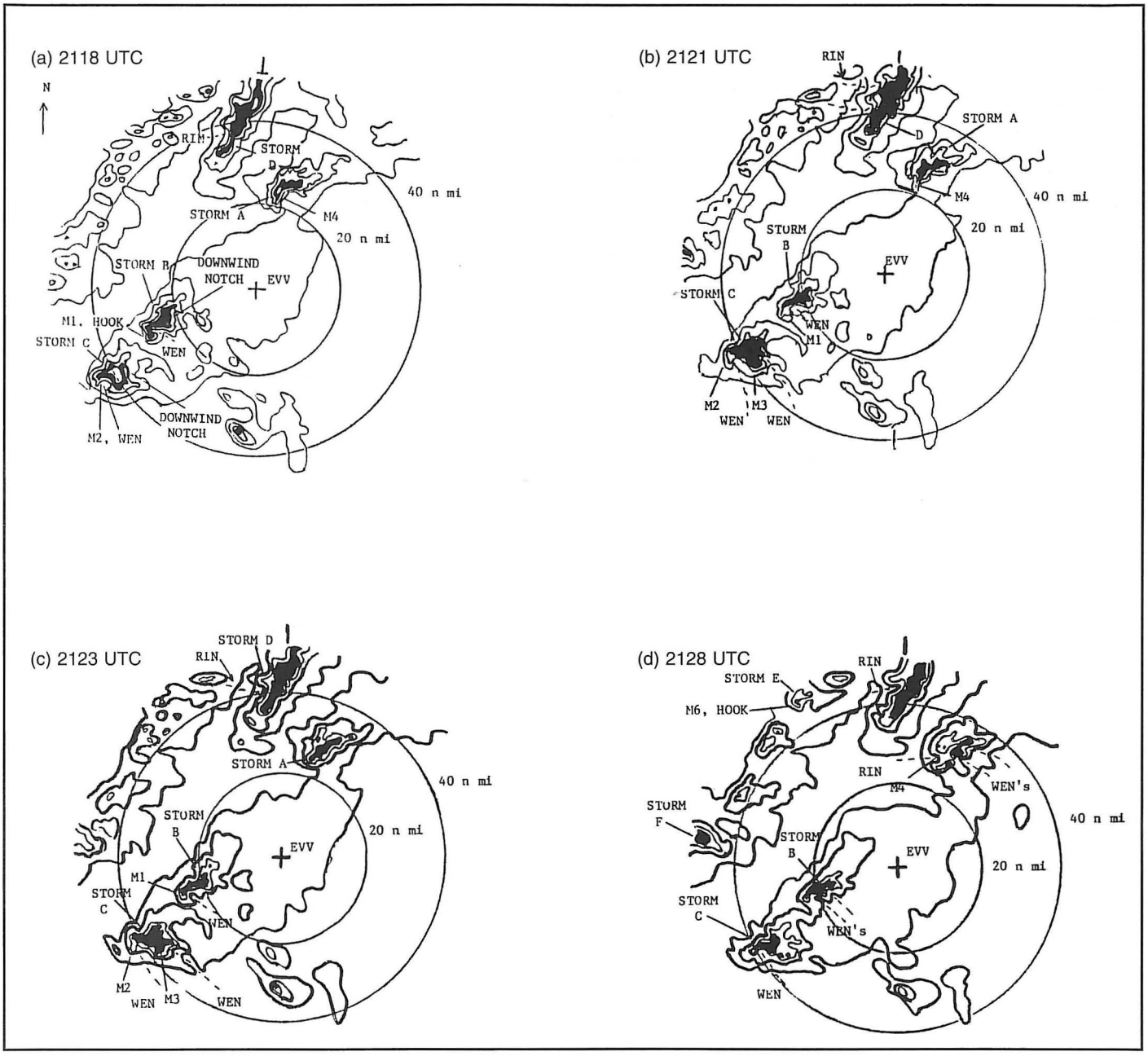

Fig. 9a-d. Time sequence of selected low-level reflectivities from 2118 to 2128 UTC. Elevation angle was set at 0.5°. VIP levels 1–5 are contoured and VIP level 4 is shaded in black. M1–M4 denotes suggested mesocirculations, including hook echoes. WEN signifies weak echo notches and RIN signifies rear inflow notches.

over 50 HP supercells during the period 1973 to 1990. Also, Nelson (1987) and Przybylinski et al. (1993) found evolution of supercells from classic to HP sometimes occurs. The mesocirculation appeared to migrate towards the center of the storm. From 2128 to 2134 UTC (Figs. 9d and 10a), multiple low-level inflow notches, indicating probable updraft centers, were observed along the leading edge of the storm. Meanwhile, a single notch along the trailing edge of the storm indicated probable descending flow at 2128 to 2134 UTC.

Storm D was located on the south end of a solid line of convection. It also exhibited HP supercell characteristics from 2118 to 2134 UTC (Figs. 9a-d and 10a) and likely produced the report of 60 mph winds at Fort Branch, Indiana located 14 n mi north of Evansville around 2140 UTC. A rear inflow notch (RIN) can be seen on the trailing flank of storm D from 2118 to 2134 UTC. This feature likely represents a region of lower equivalent potential temperature air impinging upon the line and probably reaching the surface at the leading edge of the convection as a gust front. The RIN appeared most impressive at 2128 UTC, but no additional damage was confirmed from the tail end of the line while over southwest Indiana. Additional RINs were visible after 2128 UTC (Fig. 10a-e) on the south end of the line, but were more impressive at 2151 UTC. Also, storm D had the indications of a broad and enlarged hook echo structure (M9) near the southern flank of the storm from 2139 to 2151 UTC (Fig. 10b-e). This type of echo configuration is

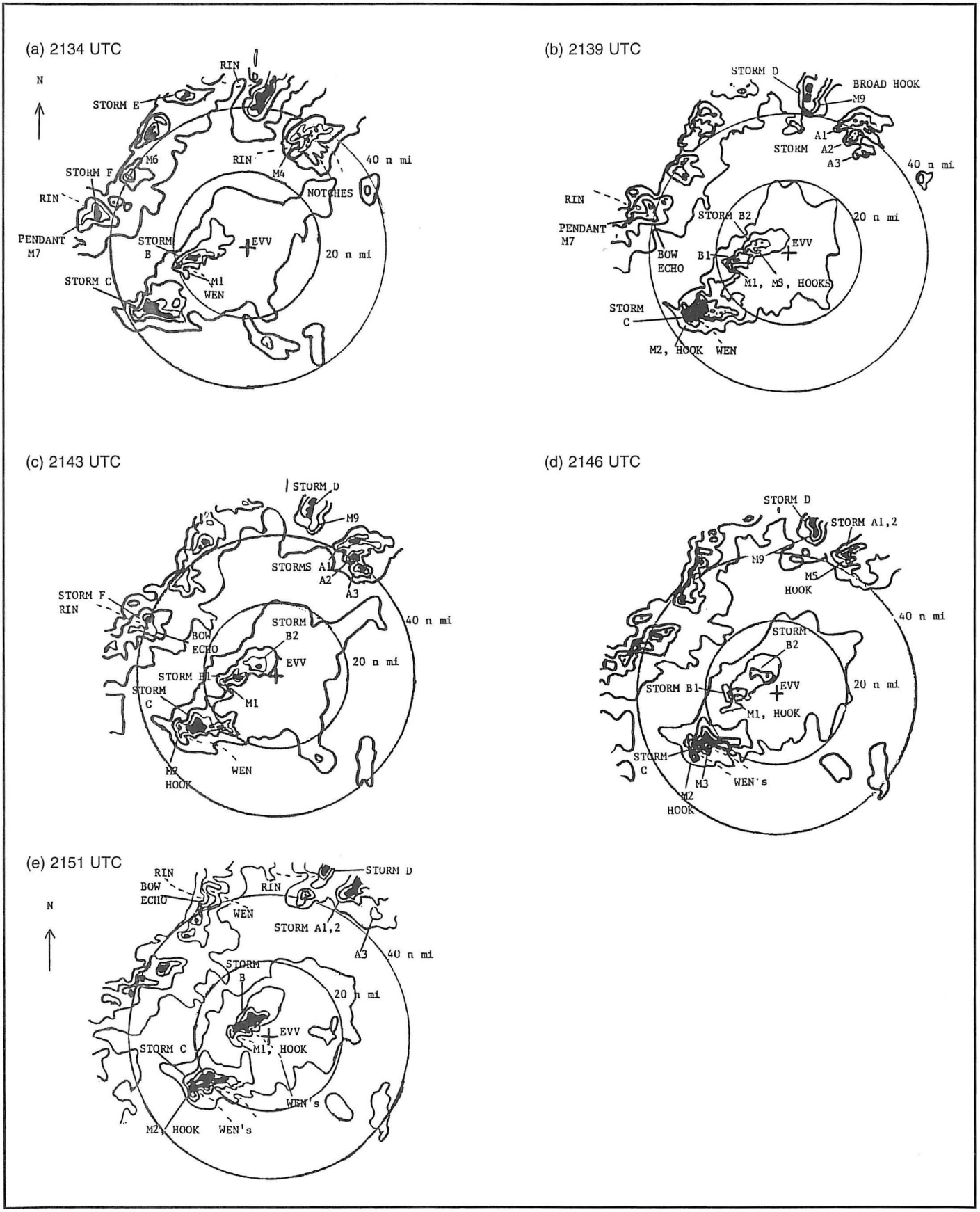

Fig. 10a-e. Time sequence of selected low-level reflectivities from 2134 to 2151 UTC. Elevation angle was set at 0.5°. VIP levels 1–5 are contoured and VIP level 4 is shaded in black. M1–M9 denotes suggested mesocirculations, including hook echoes. WEN signifies weak echo notches and RIN signifies rear inflow notches.

similar to HP storm structures documented by Moller et al. (1990). Such broad and enlarged hook echoes in HP supercells are a reflection of large weak to moderate intensity mesocyclones on the front flanks of the storm.

The VIP 3 and 4 core of storm A continued to undergo splitting from 2123 to 2139 UTC (Figs. 9d and 10a-b) to form storms A1, A2, and possibly A3. Meanwhile, the mesocirculation, M4, appeared to dissipate after 2134 UTC. By 2143 UTC, the cluster of storms A1, A2, and A3 briefly intensified with VIP 4 cores. By 2146 UTC, storm A3 weakened and storms A1 and A2 appear to merge. The core VIP 3 and 4 patterns of the storm merger formed a possible hook echo on the southwest flank, suggesting the location of a possible mesocirculation, M5. The hook echo on the southwest flank was no longer apparent by 2151 UTC. Severe weather was not confirmed from storms, A1, A2, or A3 during this period. Echo patterns during storm A's lifespan suggested the storm evolved from a classic to an HP supercell having multiple updraft centers. Similar evolution of classic to HP supercells having multiple updraft centers were found by Moller et al. (1990), Nelson (1987), and Przybylinski et al. (1993) as stated earlier in the paper.

The line of convection located 40 to 50 n mi west, northwest of Evansville did not produce severe weather from 2118 to 2151 UTC. However, a few interesting features were observed as the VIP 3 cores intensified to VIP 4. Storm E had a VIP 3 core at 2128 UTC with indications of a short-lived hook echo, M6, near the southwest flank. A subtle pendant echo continued to be observed near the southwest flank at 2134 UTC. However, the VIP 4 appeared to migrate to the forward center portion of the storm. This may indicate that M6 also translated from the southwest flank of the storm to the forward center portion of the storm. The hook was no longer distinguishable at 2139 UTC. Another storm in the line, F, had core intensities of VIP 3 and 4 at 2134 UTC. A pendant echo structure, M7, near the southwest flank and reflections of a RIN along the trailing edge of the storm were observed. By 2139 UTC, the RIN along the trailing edge became more visible, while the pendant near the southwest flank persisted. The low-level reflectivity pattern of storm F had evolved to that of a spearhead or bow echo. Such low-level reflectivity patterns have been found by Fujita (1978) and Przybylinski and Gery (1983) to indicate downburst activity, but no severe weather was confirmed from storm F. The bow shaped echo persisted through 2143 UTC, but had dissipated by 2146 UTC. A second bow shaped echo pattern became visible at 2151 UTC in the northern portion of the western-most line.

It is interesting to note that the VIP 4 core of storm B had split in two by 2134 UTC, suggesting the existence of multiple updraft centers. By 2139 UTC, the low-level reflectivity pattern suggests two seperate supercells, B1 and B2. Both storms had possible hook echoes, M1 and M8. Simultaneously, the pendant on the southwest flank of storm C had curled around to become a hook echo, M2. Thus, triple classic supercells were present on the Evansville network radar. The hook on storm B2 appeared to dissipate by 2143 UTC as the storm weakened, but a possible hook persisted through 2151 UTC on the southwest flank of B1. Storm B1 went on to produce the weak (F0) tornado at St Phillip, Indiana located 8 n mi west of Evansville at about 2150 UTC. This may have been the same tornado that touched down just northwest of Evansville about 2155 UTC. Later that evening, storm B1, may have produced a strong (F2) tornado at 0055 UTC near Washington, Indiana. Further upwind storm C continued to move northeast from about 240° at 40 kts towards Evansville. A hook or pendant persisted on the southwest flank through 2151 UTC. Additionally, weak echo notches (WENs) on the southeast flank of the storm suggested probable inflow regions and mesocirculations, M2 and M3. This storm later produced the strong (F2) tornado on the east side of Evansville about 2245 UTC (Fig. 11). Furthermore, it is believed this same storm spawned the F1 tornado in Holland, Indiana located 32 n mi northeast of Evansville at 2330 UTC.

Fig. 11. Photo looking northwest at wall cloud and F2 tornado produced by storm C on the east side of Evansville, Indiana at 2245 UTC 15 May 1986. Rain shaft of the classic supercell is visible on right side of photo, while the wall cloud and tornado are located on the southwest flank.

5. Summary

An unstable air mass with moderate wind shear provided a marginally favorable environment for severe thunderstorms and tornadogenesis on 15–16 May 1986. A pre-existing outflow boundary was produced from an MCS and provided a narrow zone of increased warm air advection and moisture convergence. The boundary provided a source of baroclinically generated horizontal vorticity which was likely tilted by the storm's updraft centers. This is one reason severe weather occurred mainly over southwest Indiana during the time examined and not along the western-most line of convection. Both the boundary and an unstable air mass are common factors linked to HP supercell development (Moller et al. 1990).

Several storms exhibited classic supercell characteristics during their lifespan, while others evolved from classic to HP supercells. Current knowledge and conceptual ideas of severe storms were supported by the low-level reflectivity features and reports of tornadoes from storms B1, B2 and C. This prompted National Weather Service personnel to issue tornado warnings in southwest Indiana, while tornado watches were already in effect for the area. Still, parent storm A and it's splitting storms failed to produce severe weather even though some classic supercell features were observed on radar. It should be remembered too that bow echo patterns were observed in the western-most line of convection, which produced no damage. Also, a short-lived hook and a pendant were observed in the same line. It's difficult to determine why severe winds did not occur with this part of the line. A few points to consider include: 1) the presence of a more stable air mass, 2) a limited spotter network over this area and/or 3) a sparsely

populated geographic region. Perhaps, the circulations in the western-most line and storm A and it's splitting storms were too weak and short-lived to produce severe weather. WENs along the forward edge and RINs along the trailing side were observed with the western-most line. The evolution of RINs and WENs associated with the supercells appeared to highlight the location of the mesocirculations near the southern flank of each storm. Such strong circulations will often redistribute the precipitation field, aiding in the evolution of such reflectivity structures. Unfortunately, radial velocity data were not available and would be needed to verify the presence of mesocyclones. Downwind notches observed on the northeast flanks of the two classic supercells suggested strong updrafts and reflectivity cores obstructing ambient flow at midlevels. Doppler radar data such as from WSR-88Ds will significantly help to alleviate some of the guess work during future severe weather operations.

Acknowledgments

Special thanks to Ron Przybylinski for reviewing my initial draft copy. He is currently the Science and Operations Officer at the St. Charles, Missouri, NWS Forecast Office. Also, thanks to Preston Leftwich of the NWS Central Region Headquarters, Kansas City, Missouri for additional review of the manuscript and to Norman Carroll, Meteorologist-in-Charge, at the Evansville, Indiana, NWS Office for checking data.

Author

John Wright currently serves as a Meteorologist at the Midwest Agricultural Weather Service Center in Lafayette, Indiana. Applied severe storms and radar research are still his prime interests. He received a B.S. degree (1978) in meteorology from Purdue University.

References

Bothwell, P.D., 1989: Forecasting Convection with the AFOS Data Analysis Programs (ADAP-Version 2.0). *NOAA Tech. Memo. NWS SR-122.* NOAA/National Weather Service Southern Region, Fort Worth, TX, 92 pp.

Brown, R.A. and K.C. Crawford, 1972: Doppler Radar Evidence of Severe Storm High Refectivity Cores Acting as Obstacles to Airflow. *Proc. 15th Wea. Radar Conf.,* Amer. Meteor. Soc., Champaign-Urbana, 16–26.

Davies, J.M., 1989: On the use of Shear Magnitudes and Hodographs in Tornado Forecasting. *Preprints, 12th Conf. Wea. Forecasting and Analysis,* Monterey, Amer. Meteor. Soc., 219–224.

Davies-Jones, R., D. Burgess and M. Foster, 1990: Test of Helicity as a Tornado Forecast Parameter. *Preprints, 16th Conf. on Severe Local Storms,* Kananaskis Park, Amer. Meteor. Soc., 588–592.

Fujita, T.T., 1971: A proposed characterization of tornadoes and hurricanes by area and intensity. *Satellite and Mesometeorology Research Project Report No. 91,* Dept. of Geophysical Sciences, Univ. of Chicago, 5734 S. Ellis Ave., Chicago, IL 60637, 42 pp.

_____, 1978: Manual of Downburst Indentification for Project Nimrod. *Smrp. Res. Paper 156,* Univ. of Chicago, 42 pp.

Hart, J.A. and J. Korotky, 1991: *The Sharp Workstation -V1.50 Users Manual.* A Skew T/Hodograph Analysis and Research Program for the IBM and Compatible P.C. NOAA/National Weather Service, Forecast Office, Charleston, WV, 62 pp.

Johns, R.H., J.M. Davies, and P.W. Leftwich, 1990: An Examination of The Relationship of 0–2 KM Ag "Positive" Wind Shear to Potential Buoyant Energy in Strong and Violent Tornado Situations. *Preprints, 16th Conf. Severe Local Storms,* Kananaskis Park, Amer. Meteor. Soc., 593–598.

Klemp, J.B., 1987: Dynamics of Tornadic Thunderstorms. *Ann. Rev. Fluid Mech.* 369–402.

Lilly, D.K., 1986: The Structures, Energetics, and Propagation of Rotating Convective Storms. Part II: Helicity and Storm Stabilization. *J. Atmos. Sci.,* 43, 126–140.

Miller, R.C., 1972: The Notes on Analysis and Severe Storm Forecasting Procedures of the Air Force Global Weather Central. *Tech. Rpt. 200,* 1050–1124.

Maddox, R.A., Hoxit L.R., and C.F. Chappell, 1980: A Study of Tornadic Thunderstorm Interactions with Thermal Boundaries. *Mon. Wea. Rev.,* 108, 322–336.

Moller, A.R., C.A. Doswell III, and R.W. Przybylinski, 1990: High Precipitation Supercells: A Conceptual Model and Documentation. *Preprints, 16th Conf. Severe Local Storms,* Kananaskis Park, Amer. Meteor. Soc., 52–57.

National Oceanic and Atmospheric Administration, 1986: National Climatic Data Center, Ashville, NC, *Storm Data,* Vol. 28, No. 5, pp 26–27, 31–32, 34, and 44.

Nelson, S.P., 1987: The Hybrid Multicellular-Supercellular Storm-An Efficient Hail Producer Part III: General Characteristics and Implication For Hail Growth. *J. Atmos. Sci.,* Vol. 44, 15, 2060–2073.

Przybylinski, R.W. and W.J. Gery, 1983: The Reliability of the Bow Echo as an Important Severe Weather Signature. *Preprints, 13th Conf. Severe Local Storms,* Tulsa, Amer. Meteor. Soc., 270–273.

_____, J.T. Snow, E.M. Agee, and J.T. Curran, 1993: The Use of Volumentric Radar Data to Identify Supercells: A Case Study of June 2, 1990, *Proceeding Volume, Tornado Symposium III,* Amer. Geo. Union. Monograph 79, 241–250.

Schaefer, J.T. and R.L. Livingston, 1990: The Evolution of Tornado Proximity Soundings. *Preprints, 16th Conf. Severe Local Storms, Kananaskis Park,* Amer. Meteor. Soc., 96–101.

Weisman, M.L. and J.B. Klemp, 1982: The Dependence of Storm Structure on Vertical Wind Shear and Buoyancy. *Mon. Wea. Rev.,* 110, 504–520.

_____ and _____, 1984: The Structure and Classification of Numerically Simulated Storms in Directionally Varying Wind Shears. *Mon. Wea. Rev.,* 112, 2479–2498.

_____ and _____, 1986: Characteristics of Isolated Convective Storms. *In Mesoscale Meteorology and Forecasting,* P.S. Ray (Ed.), Amer. Meteor. Soc., Boston, 331–357.

Xiang, X. and S.K. Beckman, 1986: The Analysis of Surface Moisture Convergence/Divergence Fields and Severe Weather Based on Certain Satellite Cloud Patterns. *Satellite Imagery Interpretation for Forecasters,* P.S. Parke (Ed.), Natl. Wea. Assn. Monograph 2-86, Vol. 2, 4-E-1-4-E-4.